EXPERIMENTAL CHARACTERIZATION AND ADJUSTMENT OF FINITE ELEMENT MODELS OF SUBMERGED STRUCTURES

BADAN, Marco A. B. C., mabcbadan@gmail.com
Instituto Federal de Goiás - IFG, Rua 75, nº 46, centro, Coord. de Mecânica, Goiânia – GO. CEP:74055-110

RADE, Domingos A., domingos@ufu.br
Universidade Federal de Uberlândia - UFU, Av. João Naves de Ávila, 2121, Bloco 1M, Campus Santa Mônica, Uberlândia – MG - CEP 38400-902

PILLET, Emmanuel, manu.pillet@gmail.com
Universidade Federal de Uberlândia - UFU, Av. João Naves de Ávila, 2121, Bloco 1M, Campus Santa Mônica, Uberlândia – MG - CEP 38400-902

PENA, José L. O., jlop@ifg.edu.br
Instituto Federal de Goiás - IFG, Rua 75, nº 46, centro, Coord. de Mecânica, Goiânia – GO. CEP:74055-110

Abstract. *This paper investigates procedures for testing vibration of small beams and plates in laboratory under the hypothesis of a stationary surrounding fluid. They are used for experimental characterization of the influence of fluid on the structural dynamic responses. It is also proposed a simplified procedure for modeling the influence of the fluid on the dynamic behavior, based on an updating procedure of finite element models. The test items are fixed on the side of a box of carbon steel, designed for this purpose, where the experimental tests are carried out with impact excitation. They are tested without and with fluid interaction. Numerical simulations of finite element models of these structures are generated in order to obtain temporal and harmonic responses for the two conditions. All sets of responses are compared and a procedure is used to update models by the correction parameters of mass and / or stiffness from the minimization of differences between the numerical and experimental eigensolutions. The results lead to global correction factors that allow to characterize the influence of the fluid in the modeling of the structures. The study highlights the computational advantage obtained in terms of processing, objectivity (given the fact that commercial software simulation of fluid does not deal with structural dynamics) and in improving the predictive ability of finite element models.*

Keywords: *Model updating; Finite elements; Dynamic characterization; Fluid structure interaction*

1. INTRODUCTION

The need to model the problems involving more than one physical domain with quality and accuracy, also called coupled problems, has become a frequent reality. Even with powerful tools and sophisticated computational modeling methods, solving problems involving interactions between different physical domains is a very complex task. Among these, the problems of fluid interaction with structures are placed among the most challenging ones, frequently involving practical applications, like oil exploration in deep water, pipelines, cables and moorings at the seabed.

It is understood by Fluid Structure Interaction (FSI) any situation in which there is some kind of fluid acting internally or externally with any movable or elastically deformable structure, affecting or influencing, directly or indirectly the movement of the latter (BUNGARTZ; SCHÄFER, 2006). The FSI problems do not fit in the classical problems of fluid mechanics because the obstacles are considered rigid (non-deformable barriers) and the focus is the study of Fluid Dynamics, even if they are affected by the presence of solid bodies. Similarly, the FSI does not fit the classic study of Strength of Materials and Structural Dynamics, where the static and dynamic are formulated independently of the surrounding fluid.

Solving techniques based on numerical methods have been used as an important tool in different areas, either in science or in engineering. The models and methods can provide reliable answers which can be quite close to experimental observations. Numerically, the problems of FSI are treated based on two main lines of research:

- One line establishes physical domains occupied by the structure and by the fluid when there is flow, or by the formulation based on added mass when the fluid is at rest.
- Another line establishes a fictitious domain for the structure, where the problems are formulated based on the principles of immersed boundary.

The physical domain approach separates the problem into three subsystems: the fluid, structure and boundary. This approach assumes the need for "communication between domains" since the equations governing the two areas have different reference systems. The principle is to make the temporal evolution of the problem until a local convergence in one area and then pass the variables to the other domain through the conditions of engagement. This line of approach is widely used because it takes into account the mutual effects between the two subdomains. This concept is also called two-way coupling. (CASADEI; Halleux, 1995) (KVAMSDAL et al., 1999a), (KVAMSDAL et al., 1999b), (PADOVESE, 2001), (WADHAM-GAGNON et al., 2007).

Another simplified way of analyzing the problems of FSI is to obtain the response of the fluid assuming a rigid structure and then the response of the structure considering the pressure interface acting as the external load. This concept is called one-way (TEIXEIRA, 2001). However, this unbound procedure can lead to very large errors if the hypothesis of stationarity for the fluid is not fulfilled.

The method of added mass (defined as "one way") is interesting because it allows the investigation of the dynamics of the structure without determining the fluid motion and hence reducing the computational cost. Added mass is usually calculated assuming a perfectly static fluid with low amplitudes in structural movement so as not to induce motion in the fluid. Historically, Meyerhoff (1970, *apud* ERGIN; UGURLU, 2003) calculated the added mass to thin bars in an infinite fluid and described the potential flow around the bar. Liang (2001 *apud* ERGIN; UGURLU, 2003) adopted an empirical formula for added mass to determine the frequency and modes of submerged bars, comparing with numerical predictions (CONCA et al., 1997).

In the context describe above, the present paper aims at proposing and performing test procedures of vibration on small submerged structures in laboratory for the experimental characterization of the influence of fluid on the structural dynamic response (time, harmonic and modal responses). Moreover, it intends to perform the assessment of a simplified procedure for modeling the influence of fluid on the structural dynamic behavior based on a updating procedure of finite element models.

2. MODELING OF FLUID STRUCTURE INTERACTION

Axisa (2001) says that for a vibrating structure under the action of an incompressible fluid, the inertial effect is immediately noticeable. The movement of the walls of the structure against a certain mass of fluid promotes the increase of the kinetic energy of the coupled system. This effect is due to the mass of the fluid which adds inertia to the system. However, depending of the geometry, of the deformable conditions and vibration conditions, the mass effect may be larger or smaller than the actual physical mass of the fluid on the structure.

2.1 Inertial effects

As a first step towards establishing the mathematical basis for the formulation of the problem, the equations of motion for structural dynamics are written in the general form:

$$[M]^E\{\ddot{x}(t)\}^E + [C]^E\{\dot{x}(t)\}^E + [K]^E\{x(t)\}^E = \{f(t)\}^E \tag{1}$$

where $[M]^E \in R^{NxN}$ is the symmetric mass matrix, positive definite, $[K]^E$ and $[C]^E \in R^{NxN}$ are the symmetric stiffness and damping matrices and they can be positive or semi-positive definite, $\{x(t)\}^E \in R^N$ is the vector of responses and $\{f(t)\}^E \in R^N$ is the vector of excitations or loads by external forces by the fluid, acting on surface structure. The superscript $(\ )^E$ makes reference to structure and the superscript $(\ )^F$ will be referred to the fluid.

Under the premise of inviscid and incompressible fluid, the Euler’s equations which are a peculiarity of the Navier and Stokes’s equations are used:

$$\vec{\nabla} \cdot \vec{V}^F = \frac{\partial V^F{}_i}{\partial x_i} = 0 \tag{2}$$

$$\rho \frac{\partial \vec{V}^F}{\partial t} + \rho \vec{V}^F \cdot \vec{\nabla} \vec{V}^F + \vec{\nabla} P = 0 \tag{3}$$

being $\vec{V}$ the velocity vector, ρ the fluid density and P the pressure.

In the case of small oscillations of the fluid, the following conditions of engagement can be specified:

$$\vec{\nabla} P \cdot \vec{n} = \rho^F \ddot{\vec{x}}^E \cdot \vec{n} = -\vec{f}^E(t)/vol \tag{4}$$

$$\vec{V}^F \cdot \vec{n}\Big|_\gamma = \vec{V}^E \cdot \vec{n}\Big|_\gamma = \dot{\vec{x}}^E \cdot \vec{n}\Big|_\gamma \tag{5}$$

$$P\big|_S = 0 \tag{6}$$

being $\vec{n}$ the unit vector in the normal direction of the interface; $\big|_\gamma$ denotes the border region and $\big|_S$ denotes the free surface.

Equation (4) indicates that the force variation due to fluid pressure on the wet wall is proportional to the acceleration imposed by the structure, while Equation (5) indicates that the fluid velocity, normal to the wet wall is equal to the normal speed of the structure at the same point, Equation (6) states that the pressure at the free surface is zero.

By introducing the condition given by Eq. (4) into Eq (1) and performing the spatial discretization, we obtain the equation of structural dynamics under the influence of fluid pressure field.

$$([M]^E + [m]^F)\{\ddot{x}(t)\}^E + [C]^E\{\dot{x}(t)\}^E + [K]^E\{x(t)\}^E = 0 \tag{7}$$

Under the simplified conditions adopted and under the appropriate boundary conditions, this expression illustrates the effect of added mass due to fluid in the mass matrix of the structure.

3. FINITE ELEMENT MODEL UPDATING

We must consider that the modeling of complex problems involve many uncertainties, which may affect the predictive ability of models. Indeed, in many circumstances, the values of physical and geometrical parameters of the system are unknown or poorly estimated; in fact, the model may involve simplifications of the real behavior. Among the technics used for the adjustments of finite element models, those based on corrections in the values of physical and geometrical parameters are considered as being among the most robust and efficient (FRISWELL; MOTHERSHEAD, 1995).

Essentially, the techniques of parametric correction involve hybrid numerical-experimental procedures and can be implemented in accordance with the following steps:

1) Perform a vibration test on the actual structure and extracting a set of dynamic features that will be used in the updating procedure.
2) Division of the model in areas to which are assigned correction factors for mass and/or stiffness and/or damping to be determined.
3) Formulation of an optimization problem in which the objective function represents the difference between the experimental dynamic features and their counterparts provided by the corresponding finite element model; the design variables are the values of the correction parameters.
4) Resolution of the optimization problem to determine the optimal values of correction parameters.

To take into account the fact that the experimental data are inevitably contaminated by measurement error, the parametric identification can be conducted in a probabilistic context. Moreover, the adjustment procedures operate on two distinct sets of data with specific techniques for comparison and compatibilization. The following presents the fundamentals the formulation of a adjustment technique based on eigensolutions (natural frequencies and natural modes of vibration) (FRISWELL; MOTHERSHEAD, 1995).

The adjustment consists basically in to establishing:

$$[M] = [M^{(0)}] + [\Delta M] \tag{8}$$

$$[K] = [K^{(0)}] + [\Delta K] \tag{9}$$

$$[C] = [C^{(0)}] + [\Delta C] \tag{10}$$

where:

- $[M],[K],[C]$ are, respectively, the matrices of mass, stiffness and damping of the model updated.
- $[M^{(0)}],[K^{(0)}],[C^{(0)}]$ are, respectively, the matrices of mass, stiffness and damping of the original model.
- $[\Delta M],[\Delta K],[\Delta C]$ are, respectively, the correction matrices of mass, damping and stiffness.

The problem consists in determining the correction matrices which reproduce, to the maximum accuracy, the dynamic responses observed experimentally. Assuming that the finite element model is undamped, the adjustment will be made on the matrices of mass and stiffness, based on values of natural frequencies obtained experimentally. It is also assumed that the finite element model has been conceived as the combination of *n_r* regions (called macro elements) to which are associated mass and stiffness correction parameters. Thus we can write:

$$\left[M^{(0)}\right]=\sum_{i=1}^{n\_r}\left[M_i^{(0)}\right] \tag{11}$$

$$\left[K^{(0)}\right]=\sum_{i=1}^{n\_r}\left[K_i^{(0)}\right] \tag{12}$$

$$\left[\Delta M\right]=\sum_{i=1}^{n\_r}m_i\left[M_i^{(0)}\right] \tag{13}$$

$$\left[\Delta K\right]=\sum_{i=1}^{n\_r}k_i\left[K_i^{(0)}\right] \tag{14}$$

where $\left[M_i\right]$, $\left[K_i\right]$ are respectively the mass and stiffness matrices associated with the *i*-th region of the global finite element model.

After parameterization of the modeling errors, we must determine the set of values of correction parameters. To formulate the problem mathematically, we use linearized Taylor series which allow relating the two data sets as follows:

$$\lambda_j^{(e)}=\lambda_j^{(m)}+\sum_{i=1}^{n\_r}\frac{\partial\lambda_j^{(m)}}{\partial m_i}\Delta m_i+\sum_{i=1}^{n\_r}\frac{\partial\lambda_j^{(m)}}{\partial k_i}\Delta k_i \tag{15}$$

where the superscript $^{(e)}$ and $^{(m)}$ designate, respectively, the experimental eigensolutions and those associated to the finite element model.

Deriving the equation that expresses the eigenvalue problem and normalization of the eigenvectors associated with the finite element model, we get the following expressions for the derivatives of eigenvalues with respect to the correction parameters (RADE, 1994):

$$\frac{\partial\lambda_j^{(m)}}{\partial m_i}=-\lambda^{(m)}\left\{\varphi_j^{(m)}\right\}^T\frac{\partial[M]}{\partial m_i}\left\{\varphi_j^{(m)}\right\}=-\lambda^{(m)}\left\{\varphi_j^{(m)}\right\}^T\left[M_i^{(0)}\right]\left\{\varphi_j^{(m)}\right\} \tag{16}$$

$$\frac{\partial\lambda_j^{(m)}}{\partial k_i}=\left\{\varphi_j^{(m)}\right\}^T\frac{\partial[K]}{\partial k_i}\left\{\varphi_j^{(m)}\right\}=\left\{\varphi_j^{(m)}\right\}^T\left[K_i^{(0)}\right]\left\{\varphi_j^{(m)}\right\} \tag{17}$$

Since we have determined the partial derivatives of eigenvalues with respect to correction parameters and having (*p*) experimental eigenvalues, from Eq. (15) we can form the following set of equations

$$\begin{Bmatrix}\lambda_1^{(e)}-\lambda_1^{(m)}\\ \lambda_2^{(e)}-\lambda_2^{(m)}\\ \vdots\\ \lambda_p^{(e)}-\lambda_p^{(m)}\end{Bmatrix}=\begin{bmatrix}\frac{\partial\lambda_1^{(m)}}{\partial m_1} & \frac{\partial\lambda_1^{(m)}}{\partial m_2} & \cdots & \frac{\partial\lambda_1^{(m)}}{\partial m_{n\_r}} & \frac{\partial\lambda_1^{(m)}}{\partial k_1} & \frac{\partial\lambda_1^{(m)}}{\partial k_2} & \cdots & \frac{\partial\lambda_1^{(m)}}{\partial m_{n\_r}}\\ \frac{\partial\lambda_2^{(m)}}{\partial m_1} & \frac{\partial\lambda_2^{(m)}}{\partial m_2} & \cdots & \frac{\partial\lambda_2^{(m)}}{\partial m_{n\_r}} & \frac{\partial\lambda_2^{(m)}}{\partial k_1} & \frac{\partial\lambda_2^{(m)}}{\partial k_2} & \cdots & \frac{\partial\lambda_2^{(m)}}{\partial m_{n\_r}}\\ \vdots & \vdots & \vdots & \vdots & \vdots & \vdots & \vdots & \vdots\\ \frac{\partial\lambda_p^{(m)}}{\partial m_1} & \frac{\partial\lambda_p^{(m)}}{\partial m_2} & \cdots & \frac{\partial\lambda_p^{(m)}}{\partial m_{n\_r}} & \frac{\partial\lambda_p^{(m)}}{\partial k_1} & \frac{\partial\lambda_p^{(m)}}{\partial k_2} & \cdots & \frac{\partial\lambda_p^{(m)}}{\partial m_{n\_r}}\end{bmatrix}\begin{Bmatrix}\Delta m_1\\ \Delta m_2\\ \vdots\\ \Delta m_{n\_r}\\ \Delta k_1\\ \Delta k_2\\ \vdots\\ \Delta k_{n\_r}\end{Bmatrix} \tag{18}$$

or

$$\{\Delta\lambda\}=[S]\{\Delta\theta\} \tag{19}$$

where $\left[S\right]$ is known as the sensitivity matrix of eigenvalues and $\left\{\Delta\theta\right\}$ is the vector formed by the increments of the parameters.

In principle, the resolution of this system of equations enables to determine the increments of the parameters that should be applied to the initial model. Because the matrix is generally not square, we use the resolution by the method of least squares.

$$\left\{\Delta\theta\right\}=\left(\left[S\right]^T\left[S\right]\right)^{-1}\left[S\right]^T\left\{\Delta\theta\right\} \tag{20}$$

However, this solution does not directly provide satisfactory results, since the linearization performed in Eq. (15) may not be applicable in cases where the corrections are not infinitesimal. Thus, an iterative resolution scheme must be used which, starting from the initial model, successive increments are calculated in such a way that at each iteration the sensitivity matrix and the eigenvectors calculated by the finite element model are updated in accordance with:

$$\Delta\{\theta\}_i=\left(\left[S(\{\theta\}_i)\right]^T\left[S(\{\theta\}_i)\right]\right)^{-1}\cdot\left[S(\{\theta\}_i)\right]^T\cdot\Delta\lambda(\{\theta\}_i) \tag{21}$$

$$\{\theta\}_{i+1}=\{\theta\}_i+\{\Delta\theta\}_i \tag{22}$$

where *i* indicates the *i*-th iteration. A convergence criterion based on the amplitude of the vector of increments of parameters is used to stop the iterative procedure.

Equation (21) expresses the weighting of all measures in an equivalent manner. However, there may be differences in reliability levels that are attributed to the different measures. This difference in reliability can be considered in the minimization process by a diagonal matrix $\left[W_s\right]$, positive definite, which allows to account for the degree of confidence or uncertainty to the measured data. Reliable results have small variances, hence, larger weight in the diagonal elements of the array $\left[W_s\right]$. Thus the equation (21) can be rewritten, incorporating the variation of weights:

$$\left\{\Delta\theta\right\}_i=\left(\left[S\left(\left\{\theta\right\}_i\right)\right]^T\left[W_S\right]\left[S\left(\left\{\theta\right\}_i\right)\right]\right)^{-1}\left[S\left(\left\{\theta\right\}_i\right)\right]^T\left[W_S\right]\left\{\Delta\lambda\left(\left\{\theta\right\}_i\right)\right\} \tag{23}$$

In most practical cases, the number of parameters needed to update is greater than the number of data acquired experimentally. It happens because some parameters are better estimated than others. These factors make their solution very sensitive to errors in the data. So it is performed an additional ponderation on the parameters, by a matrix $\left[W_\theta\right]$ for the regularization of the problem. The weight matrix $\left[W_\theta\right]$ is a diagonal matrix element usually chosen as the variances of the parameters. Equation (23) shall be written as:

$$\left\{\Delta\theta\right\}_i=\left(\left[S\left(\left\{\theta\right\}_i\right)\right]^T\left[W_S\right]\left[S\left(\left\{\theta\right\}_i\right)\right]+\left[\left[W_\theta\right]\right]\right)^{-1}\left[S\left(\left\{\theta\right\}_i\right)\right]^T\left[W_S\right]\left\{\Delta\lambda\left(\left\{\theta\right\}_i\right)\right\} \tag{24}$$

Alternatively, may improve the conditioning of the equations using an initial estimate of unknown parameters.

$$\left\{\theta\right\}_{i+1}=\left\{\theta\right\}_i+\left(\left[S\left(\left\{\theta\right\}_i\right)\right]^T\left[W_S\right]\left[S\left(\left\{\theta\right\}_i\right)\right]+\left[W_\theta\right]\right)^{-1}\left[S\left(\left\{\theta\right\}_i\right)\right]^T\left[W_S\right]\left\{\Delta\lambda\left(\left\{\theta\right\}_i\right)\right\}-\left[W_\theta\right]\left(\left\{\theta\right\}_i-\left\{\theta\right\}_0\right) \tag{25}$$

where $\left\{\theta_0\right\}$ is the vector of initial estimates of parameters.

Infantes (2000) comments that the analytical and experimental natural frequencies need to refer to the same mode. Sorting them in ascending order according to the values of natural frequencies may not be suitable. The use of criteria such as MAC (Modal Assurance Criterion), between the experimental and analytical modes ensures the correspondence.

4. METHODOLOGY OF EXPERIMENTAL TESTS

A box of carbon steel was constructed with internal dimensions of 550 mm x 450 mm x 410 mm, using commercial plate of ½" of thickness at the base and one side (see Figure 1). To provide better visualization of the experiment, two glass sheets were mounted on opposite sides. For closing of the box, it was mounted a plate of ¼ "on the side opposite the steel ½" of thick.

Performing the function of the beam, it was used a steel bar with free dimensions: 376.0 mm x 30.5 mm x 4.7625 mm (3/16"), clamped on one side of the box, as shown in Figure 1. As instrumentation, a piezoelectric accelerometer was set at the free end. The beam condition was evaluated in dry and submerged conditions with 180 mm of water on the upper surface and 190 mm in the lower face. The test consisted of successive applications and measurement of impulsive forces on five points distributed on its upper surface, and the response at the point where the accelerometer was positioned. At each point were performed 15 impacts to obtain the average for the FRF.

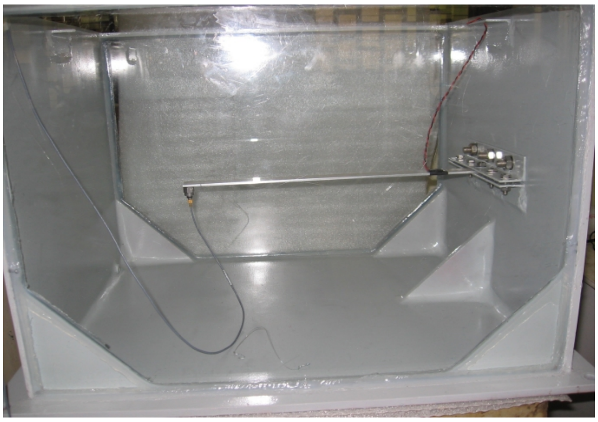

Figure 1 - Steel beam clamped with fixed instrumentation in the box.

We used a steel plate with free dimensions: 376.0 mm x 200.0 mm x 3.175 mm (1/8”), clamped on the side of the box. Also set up an accelerometer in one corner of the free end of the plate in dry and submerged conditions with 180 mm of water on the upper surface and 190 mm in the lower face. The test consisted of impulsive forces at 25 points on its upper surface. At each point were performed 15 impacts to obtain the average for the FRF.

For both structures, the tests were performed as follows:

1) Dry condition, using impact hammer in the original configuration, shown in Figure 2-a
2) On the submerged condition, using impact hammer with extended tip (Fig. 2-b)

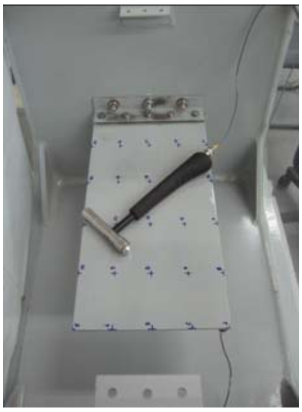

(a)

(b)

Figure 2 - Tests performed: (a) without fluid and with normal hammer.
(b) with fluid, using hammer with extended tip.

5. RESULTS AND DISCUSSION

5.1 Beam without fluid

The dynamic behavior of the beam is compared to equivalent numerical models for validation and implementation of the methodology of the model updating. The numerical models were generated in ANSYS software, using 10 elements type Beam3 with modal and harmonic analyses in the range 0 to 500 Hz. It was also implemented a finite element model in MATLAB with 10 unidimensional elements. The natural frequencies and damping factors were identified from the experimental FRFs using MODAN - *Modal Analisys Software*, version 3, developed by the *Laboratoire de Mécanique Appliquée, Université de Franche-Comté, in Besançon - France*. This is an interactive program for modal identification, developed in MATLAB that allows the extraction of eigenvalues, eigenvectors and modal damping factors from frequency response functions. The model in ANSYS was updated using the program AESOP or *Analytical or Experimental Structural Optimization Platform*, version 5, also of the *Université de Franche-Comté, France*. It is also a program developed in MATLAB for simulation, comparison of responses, localization of modeling errors, model updating, sensitivity analysis, statistics and manipulation of FRFs.

After the tests with the dry structure, differences were observed between the natural frequencies of the numerical model and their experimental counterparts. Using the technique of adjustment describe in Section 3, we obtained the global factor for the correction of the bending stiffness *0.7498 * EI* for the model in ANSYS and *0.7604 * EI* for the model developed in MATLAB. Table 1 consolidates the data obtained before and after the model updating.

Table 1 - Comparison of results: experimental, without and with update using the global stiffness

	Natural frequencies (Hz) / error (%)				
MODE	**Experim**	**ANSYS/AESOP**		**MATLAB**	
		Without	With Update	Without	With Update
1º	24,47	28,30/15,65	24,50/0,13	28,15/15,04	24,54/0,29
2º	153,96	177,31/15,17	153,54/-0,27	176,39/14,57	153,82/-0,09
3º	429,15	496,32/15,65	429,78/0,15	494,05/15,12	430,81/0,39

The differences observed between the results with AESOP/ANSYS and MATLAB are attributed to the choice of objective function, weighting of the modes and characteristics inherent of the numerical optimization.

For further evaluation, the amplitudes of FRFs obtained experimentally with the corresponding generated by harmonic analysis in ANSYS from the fitted model using the program AESOP are compared in Figure 3. The modal damping factors identified experimentally were introduced in the updated finite element model.

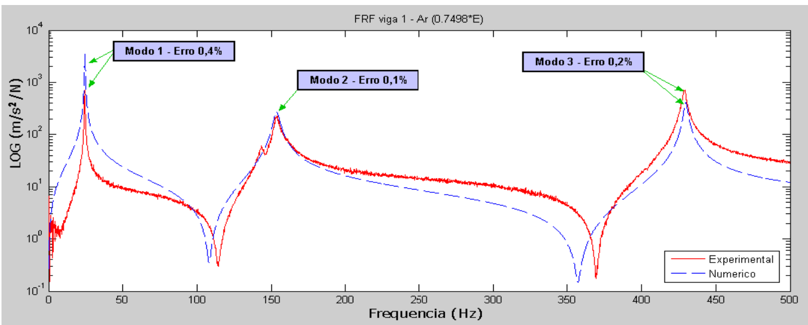

Figure 3 -FRF for the dry beam

5.2 Beam in interaction with fluid

Similar testing and updating procedures were used for the submerged structure. The best results were obtained by making a direct correction from the original model, avoiding the previous correction by stiffness, using the global mass correction factor for all elements of the model. They were obtained $2{,}166 * \rho$ for the model in ANSYS and $2{,}076 * \rho$ for the model in MATLAB. Table 2 consolidates the data obtained before and after model updating.

Table 2 - Comparison of results: Experimental, without and with update using the global mass on submerged beam

MODE	Natural frequencies (Hz) / error (%)				
	Experim	ANSYS/AESOP		MATLAB	
		Without	With Update	Without	With Update
1º	19,17	28,30/15,65	19,23/+0,31	28,15/46,84	19,14/-0,16
2º	119,80	177,31/15,17	120,48/+0,57	176,39/47,24	120,05/0,21
3º	337,86	496,32/15,65	337,24/-0,17	494,05/46,23	337,07/-0,23

The amplitudes of FRFs obtained experimentally with the corresponding generated by harmonic analysis in ANSYS from the adjusted model are compared in Figure 4.

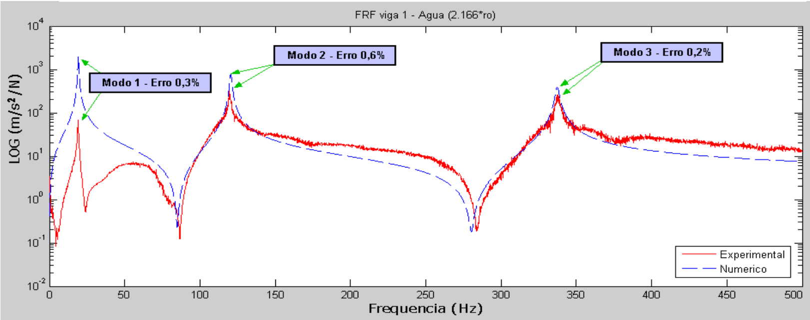

Figure 4 - FRF for the submerged beam

In Figure 4 it can be seen that the experimental curve present some noise which can be due to fluid motion induced by the structure. It should also be pointed-out that the excitation of the structure under water, along with the instrumentation that was available, was one of the difficulties encountered in performing this work.

5.3 Plate without fluid

A numerical model was generated with 760 Shell63 elements in ANSYS, with modal and harmonic analyses performed in the range 0 to 1000 Hz. The natural frequencies and damping factors were also identified using MODAN and updating was made using AESOP/ANSYS.

The differences between the natural frequencies of the numerical model and the experimental data were minimized using the updating technique using the global correction factor of *0.782 * EI* for the bending stiffness on the model in ANSYS. Table 3 consolidates the data before and after the model updating.

Table 3 - Comparison of results: experimental, without and with update using the global stiffness on plate without fluid

MODE	Natural frequencies (Hz) / error (%) / MAC(%)		
	Experim.	**Before Updating**	**After Updating**
1º	16,76	19,26/+14,92/ 99,8	17,03/+1,61/ 99,8
2º	70,69	78,61/+11,20/ 99,4	69,51/-1,67/ 99,4
3º	104,91	119,99/+14,37/ 98,8	106,11/+1,14/ 98,8
4º	229,96	257,71/+12,07/ 99,4	227,90/-0,90/ 99,4
5º	296,64	336,29/+13,37/ 97,8	297,39/+0,25/ 97,8
6º	425,51	464,91/+9,26/ 72,3	411,13/-3,38/ 72,3
7º	446,90	500,95/+12,09/ 69,3	443,00/-0,87/ 69,3
8º	574,19	---	NU
9º	591,14	675,88/+14,34/ 65,8	597,70/+1,11/ 65,8
10º	731,06	835,91/+14,34/ 96,1	739,22/+1,12/ 96,1
11º	843,22	936,94/+11,11/ 89,6	828,56/-1,74/ 89,6
13º	951,13	1107,68/+16,46/ 92,9	979,55/+2,99/ 92,9

NU = Not Updated

Figure 5 enables to compare the amplitudes of FRFs obtained experimentally and the corresponding generated by harmonic analysis performed in ANSYS from the updated model using the program AESOP.

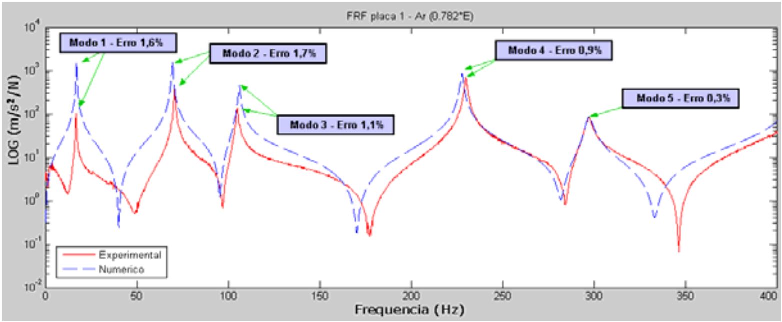

Figure 5 - FRF for the dry plate (range of 0 to 400 Hz)

The FRFs of the updated model are compared with the experimental FRF's showing similarities in the appearance of curves. It is observed that the correlation between numerical and experimental methods was better from 0 to 400 Hz.

5.4 Plate in interaction with fluid

Similar procedure was applied to the submerged plate. The best updating results were obtained by direct correction of the model without correction for the stiffness and using the global factor to the mass. It was obtained a factor of $4{,}40 * \rho$. Table 4 consolidates the data obtained before and after adjustment models. Figure 6 enables to compare the amplitudes of FRFs obtained experimentally and the corresponding generated by harmonic analysis performed in ANSYS from the updated model.

Table 4 - Comparison of results: Experimental, with and without adjustment of the global mass on plate submerged

	Natural frequencies (Hz) / error (%) / MAC(%)		
MODE	**Experim.**	**Before Updating**	**After Updating**
1º	7,27	19,26/+164,92/ 95,1	9,28/+27,65/ 95,1
2º	39,61	78,61/+98,46/ 84,8	37,89/-4,34/ 84,8
3º	48,60	119,99/+146,89/ 71,9	57,83/+18,99/ 71,9
4º	132,58	257,71/+94,38/ 86,2	124,22/-6,31/ 86,2
5º	146,44	336,29/+129,64/ 83,0	162,09/+10,69/ 83,0
6º	262,12	464,91/+77,37/ 74,0	224,09/-14,51/ 74,0
7º	268,27	500,95/+86,73/ 77,5	241,46/-9,99/ 77,5
8º	310,61	---	N.U.
9º	367,30	675,88/+84,01/ 54,2	N.U.
10º	446,70	835,91/+87,13/ ---	N.U.
11º	531,26	936,94/+76,36/ 56,2	N.U.
13º	539,65	1107,68/+105,26/ ---	N.U.

N.U. = Not Updated

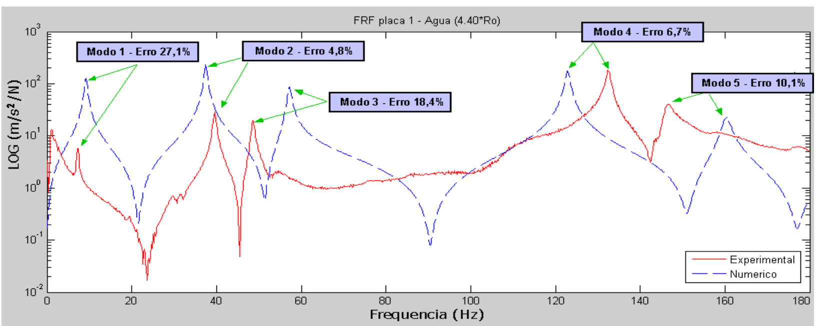

Figure 6 - FRF for the submerged plate (range of 0 to 400 Hz)

As can be seen, the values of the natural frequencies of the plate decrease due to the fluid added mass, which limits the number of modes available for adjustment, as indicated by the MAC criterion (Tab. 4). At this point, questions arise about the influence of the excitation system on the contamination of the experimental response, as discussed earlier for the beam. In the presentation of the FRFs there were residual differences between modal frequencies obtained by updating. However, there were also certain similarities between the appearance of amplitude curves, the peaks of the natural frequencies and the presence of anti-resonances, despite the apparent noise.

6. CONCLUSIONS

The simplified modeling methodology proposed in this work has shown to have potential for characterization of the structural behavior of a structure surrounded by a static fluid, requiring, however, some improvement. As proposals to continue the study reported here, we suggest: a) investigations of the means of acquiring data for the dynamics of submerged structures in terms of excitation, instrumentation, and reliability; b)study of the acceptable limits for the static condition of the fluid; c) use of updating techniques based on FRFs that preclude the step of identifying modal parameters; d) inclusion in the numerical models and adjustment procedures the effect of damping induced by fluid viscosity, which induces the decay of responses observed for submerged structures.

7. ACKNOWLEDGEMENTS

The authors express their gratituted to CAPES for financial support, to the Federal University of Uberlândia and to the Federal Institute of Goiás for the conditions offered for this work, to Minas Gerais State Research Agency FAPEMIG, for the grant of a post-doctoral scholarship to Dr. E. Pillet (Project TEC-00298/08).

8. REFERENCES

AXISA, F. **Modélisation des Systèmes Mécaniques – Interactions Fluide Structure.** Paris – France: Hermes Science Publications, 2001, Vol. III.

BUNGARTZ, H. J.; SCHÄFER, M. Fluid-Structure Interaction Modelling, Simulation, Optimisation. **Lecture Notes in Workshop of Computational Science and Engineering.** New York, v.53, 2006.

CASADEI, F.; HALLEUX, J. P. An algorithm for permanent fluid-structure interaction in explicit transient dynamics. **Comput. Methods Appl. Mech. Engrg.** v. 128, p. 231-289, Dec. 1995.

CONCA, C.; OSSES, A.; PLANCHARD, J. Added Mass and Damping in Fluid-Structure Interaction. **Computer Methods in Applied Mechanics and Engineering**. v. 146, n. 3, p. 387-405, Jul. 1997.

ERGIN, A.; UGURLU, B. Linear vibration analysis of cantilever plates partially submerged in fluid. **Journal of Fluids and Structures.** v. 17, n. 7, p. 927-939, 2003.

FRISWELL, M. I.; MOTTERSHEAD, J. E. **Finite Element Model Updating in Structural Dynamics.** London, Kluwer Acacemic Publishers, 1995. 282p.

INFANTES, J. E. C. **Ajuste de Modelos de Elementos Finitos Usando Técnicas de Estimação de Parâmetros.** 2000, 127 f. Dissertação de Mestrado - Universidade Estadual de Campinas, Campinas – SP.

KVAMSDAL, T.; JENSSEN, C. B.; OKSTAD, K. M.; AMUNDSEN, J. **Numerical Methods for Fluid-Structure Interactions of Slender Structures.** In: European Conference on Computational Mechanics, ECCM99, 1999a, München – Germany.

KVAMSDAL, T.; JENSSEN, C. B.; OKSTAD, K. M.; AMUNDSEN, J. **Fluid-Structure Interaction For Structural Design**. In: Proceedings of the International Symposium on Computational Methods for Fluid-Structure Interaction, FSI99, 1999b, Trondheim - Norway, Tapir Publishers. p. 211-238.

PADOVESE, G. C. **Determinação da rigidez e amortecimento equivalente proveniente do fluido escoando e interagindo com placas flexíveis: Teoria e constatações experimentais.** 2001. 224 f. Dissertação de Mestrado - Universidade Estadual de Campinas, Campinas – SP.

RADE, D. A. **Correction Paramétrique de Modèles Éléments Finis: Élargissement de L´Espace de Connaissance.** 1994. 203 f. Tese de Doutorado – L´Université de Franche-Comté, Besançon - France.

TEIXEIRA, P. R. F. **Simulação numérica da interação de escoamentos tridimensionais de fluidos compressíveis e incompressíveis e estruturas deformáveis usando o método de elementos finitos.** 2001. 237 f. Tese de Doutorado - Universidade Federal do Rio Grande do Sul, Porto Alegre – RS.

WADHAM-GAGNON, M.; PAIDOUSSIS, M. P.; SEMLER, C. Dynamics of cantilevered pipes conveying fluid. Part 1: Nonlinear equations of three-dimensional motion. **Journal of Fluids and Structures.** v. 23, p. 545–567, 2007.

9. RESPONSIBILITY NOTICE

The authors are the only responsible for the printed material included in this paper.